THESIS FOR THE DEGREE OF LICENTIATE OF ENGINEERING

Simulating nonlinear optical effects in periodically patterned integrated waveguides

Albin Jonasson Svärdsby

Department of Physics
CHALMERS UNIVERSITY OF TECHNOLOGY
Göteborg, Sweden 2024

Simulating nonlinear optical effects in periodically patterned integrated waveguides
Albin Jonasson Svärdsby

Department of Physics
Chalmers University of Technology
SE-412 96 Göteborg, Sweden
Telephone +46 (0)31 772 10 00

Cover: Illustration of the four wave mixing process that is used in an optical parametric amplifier, with a pump, signal, and idler frequency.

Chalmers digitaltryck
Göteborg, Sweden 2024

Simulating nonlinear optical effects in periodically patterned integrated waveguides

Albin Jonasson Svärdsby
Department of Physics
Chalmers University of Technology

Abstract

The nonlinear optical coefficients are very small for most materials. This results in a need for very long waveguides in integrated optics in order to achieve nonlinear optical processes such as optical parametric oscillation with appreciable efficiency, meter-long waveguide structures not being uncommon. This in turn makes simulations of nonlinear integrated optical devices challenging. Translationally invariant waveguides can be simulated using approximate methods such as the the beam envelope method. However, for more complicated structures, for instance a periodically patterned waveguide, these approaches becomes unfeasible. In this thesis, we describe how the nonlinear wave propagation in periodically patterned waveguides can be simulated using the nonlinear Schrödinger equation, including a computational strategy to calculate the coefficients of the nonlinear Schrödinger equation describing the linear and nonlinear effects of the optical materials. In particular, we focus on effective meshing strategies for simulations using the finite-element method and an approach to numerically determine the higher-order dispersion coefficients needed to solve the nonlinear Schrödinger equation for long, periodically patterned structures.

Keywords: Nanophotonics, nonlinear optics, FEM, parametric amplifiers, four wave mixing, OPA, FWM

LIST OF APPENDED PAPERS

This thesis is partially based on work presented in the following papers:

I **Adaptive meshing strategies for nanophotonics using a posteriori error estimation**
Albin J. Svärdsby and Philippe Tassin
Optics Express **32**, 14, pp. 24592-24602 (2024)

The author's contribution to the papers:

I Performed implementation of the method, evaluated the results and wrote the paper.

Contents

1 Introduction

The goal of this thesis is to provide the relevant theory that we need for understanding and simulating nonlinear optical effects in waveguides, with the intention of using them as optical parametric amplifiers. What this means will become clearer over the course of this thesis. We will start by setting the stage and give some examples of what these nonlinear effects can be used for and then we will dive into the theory. My assumption will be that you at a point in time have read an undergraduate course in electromagnetism or equivalent. I will repeat some core concepts of linear electromagnetics in Chapter 2 so that we are up to speed, and refresh the terminology that we will utilise on this journey. Once we are onboard, we will move over to nonlinear effects in Chapter 3 and finally treat numerical methods for how we will simulate these effects in Chapter 4.

I hope you as a reader will find the journey enlightening, and perhaps invoke some internal thoughts over the progress that is being made in the field and the interesting applications these nonlinear effects have.

1.1 What are we pursuing?

Perhaps one of the most common day-to-day appliances relying on nonlinear optics that you have come into contact with are green laser pointers. Here nonlinear effects are used to convert a 1064 nm wavelength laser source into 532 nm by means of a second-order nonlinear effect. This thesis is building towards the ability to simulate these kinds of effects for the purpose of amplifying optical signals through optical parametric processes. Amplification through nonlinear optical effects is interesting, because it enables the amplification of an optical signal with a very low noise level that can be manufactured with an on chip design [1]. Common for many of these methods is that they rely

on a rather simple geometrical layout, often consisting of some homogeneous materials or systems like Bragg gratings [2].
This geometry constraint, although it simplifies the modelling, also has the potential of excluding better designs. But complex geometries are more complicated to simulate and cannot rely on analytical solutions that can assists for well-defined and symmetric geometries. In this thesis we will provide the tools needed to simulate these kinds of structures in the context of a periodic optical waveguide structure where each unit cell in the structure can have an arbitrary pattern, as illustrated in Figure 1.1.

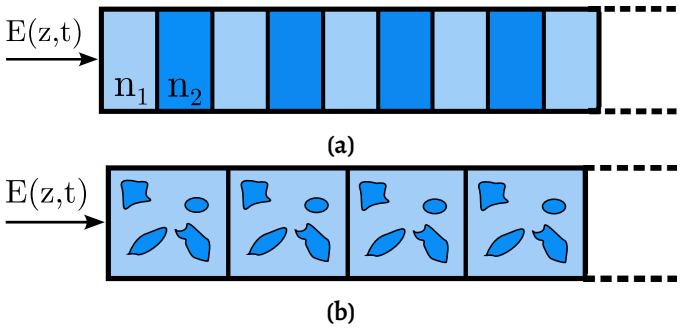

Figure 1.1: Simple vs complex geometries. Figure 1.1a shows a uniform Bragg grating, alternating between different dielectric materials. In Figure 1.1b we see an example of a more complicated geometrical shape.

2

Electromagnetic wave propagation

In this Chapter we will repeat concepts of electromagnetic wave propagation that are needed to understand the nonlinear optics and simulations that we will treat in Chapter 3 and 4. This will not be an exhaustive introduction, but should be seen more as a reminder. For people looking for a more thorough introduction to electromagnetics, see for example Griffith [3], Jackson [4] or Yariv & Yeh [5].

In section 2.1, we will treat the concept of dispersion and discuss material dependencies on frequency. This will then be followed in section 2.2 where discuss propagating modes in waveguides. Finally we will discuss periodic structures in section 2.3.

2.1 Understanding dispersion

The framework for studying the propagation of electromagnetic waves has been known for a long time, starting with the work by D'Alembert [6–8] in the 18th century continued by Euler [9] and Lagrange [10], resulting in the wave equation. The next significant description came when Maxwell presented his work of electromagnetism up to his time in 1865 [11], verified by Hertz in 1893 [12]. The Maxwell equations that we are familiar with today were however formulated by Heaviside based on the work of Maxwell [13] [14]. The macroscopic differential versions of the equations can be written as:

$$\begin{aligned} \nabla \cdot \mathbf{D} &= \rho_f, & \nabla \times \mathbf{E} &= -\frac{\partial \mathbf{B}}{\partial t}, \\ \nabla \cdot \mathbf{B} &= 0, & \nabla \times \mathbf{H} &= \mathbf{J_f} + \frac{\partial \mathbf{D}}{\partial t}. \end{aligned} \tag{2.1}$$

Anytime an electromagnetic wave interacts with a dielectric material there will be an interaction where the electric field induces electric dipole moments in the material.

These dipole moments then cause an added term to the electric field, **E**, in the form of a polarisation, **P**, and together they form what is called the displacement field [3][4]:

$$\mathbf{D} = \varepsilon_0 \mathbf{E} + \mathbf{P} = \varepsilon \mathbf{E}. \tag{2.2}$$

where the permittivities ε and ε_0 quantify the polarisation in the material and in free space, respectively. What gives rise to this effect is that a material contains both positive and negative charges, and when an electric field is applied they are pulled apart, or displaced, causing the charge distribution to be polarised. If a molecule already has a polarised distribution then the molecule also has the possibility to rotate in order to align with the applied field.

If the polarisation is the result of a field interacting with the material on a macroscopic scale, it is not unreasonable to think that this effect should be dependent on the field strength in the material and that indeed holds true. The amount of polarisation that occurs in a material when it interacts with an electric field is expressed with the electric susceptibility χ of the material 2.3

$$\mathbf{P} = \varepsilon_0 \chi \mathbf{E}. \tag{2.3}$$

When talking about dispersion, we refer to effects when the susceptibility has a frequency dependence $\chi(\omega)$. The effect of this is that waves propagating through the material have different amount of attenuation and different phase velocities depending on frequency. This results in that different frequencies travel with different speed in the material, which gives rise to things like refraction, usually illustrated with a prism like in Figure 2.1.

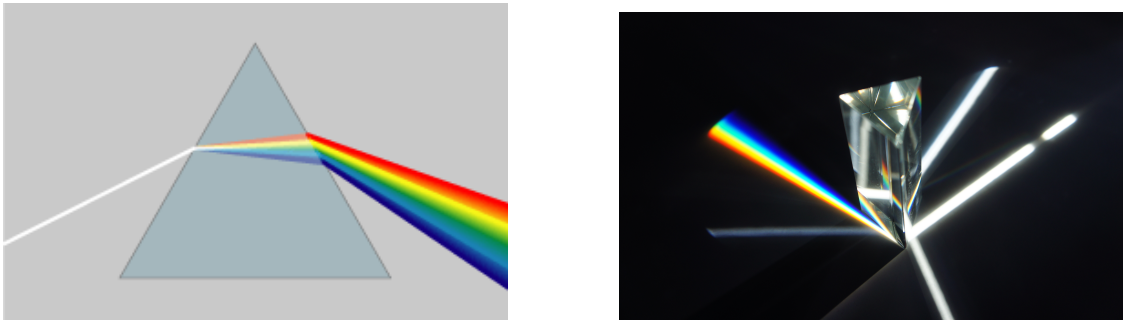

(a) (b)

Figure 2.1: Illustration of dispersion in a prism. To the left we see a 2D representation and the figure on the right we see a version in 3D.

When we are designing devices, waveguides, these linear effect have big consequences because the design needs to operate with multiple frequencies. But since we have this frequency dependence it also opens up the possibility to tailor systems and materials so that it only favour desirable frequencies and counteracts undesired ones.

2.2 Propagation modes in waveguides

When we are talking about dielectric optical waveguides, we are referring to structures that have an optical medium with high refractive index, called a core, surrounded by a material of lower refractive index, called a cladding. The purpose of the core is to confine the light and guide it along its longitudinal direction. Waveguides come in many different shapes and configurations, and readers interested in optical waveguides will do well to read Liu[15], Yariv & Yeh [5] or Saleh & Teich [16].

When we have a structure where a wave can propagate with a defined field pattern in the structure that is confined, we call it a mode. If the wave leaks out of its confinement as it propagates in the waveguide then it is a leaky mode. To illustrate what a mode is we can take the instance of a planar waveguide stretching to infinity as depicted in 2D in Figure 2.2. This type of waveguide has a fixed set of stable modes, which have has analytical solutions for the transverse field. If the solution has no electric field in the propagation direction but only in the transverse direction it is denoted as transverse electric (TE) mode. If the solution instead has no magnetic field in the propagation direction but only in the transverse direction then it is denoted as transverse magnetic (TM) mode. When we have multiple modes then we refer to them as TE0, TE1 etc. For more complex geometries, solutions involving both electric and magnetic field, so called hybrid modes are also allowed [15].

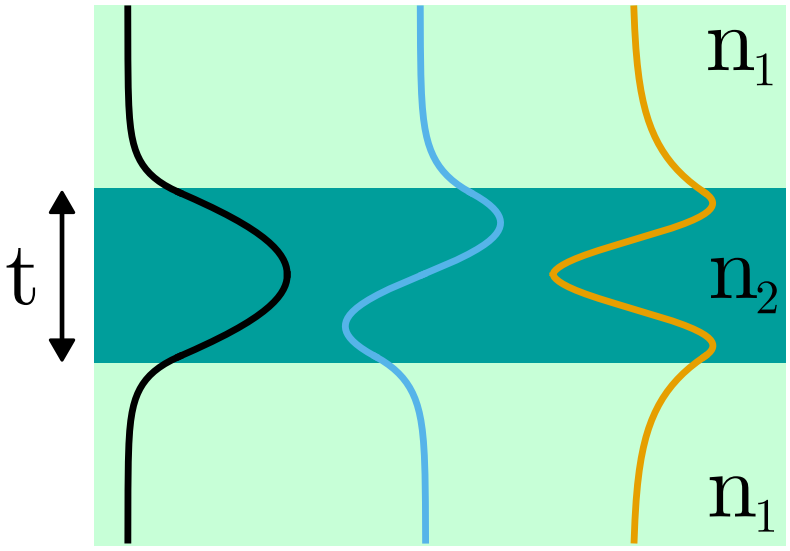

Figure 2.2: The first three propagating TE modes of a symmetric planar waveguide with dielectrics with refractive index n_1 and n_2. From left to right we see TE0, TE1, and TE2.

The different modes of the waveguide each have their own dispersion. This results in that we can express different modes on a dispersion plot as demonstrated in Figure 2.3. We can think of the modes like a change in the phase velocity of the wave due to the wave

bouncing more against the side of the waveguide, as it propagates in the longitudinal direction, as a result of different angle of incidence.

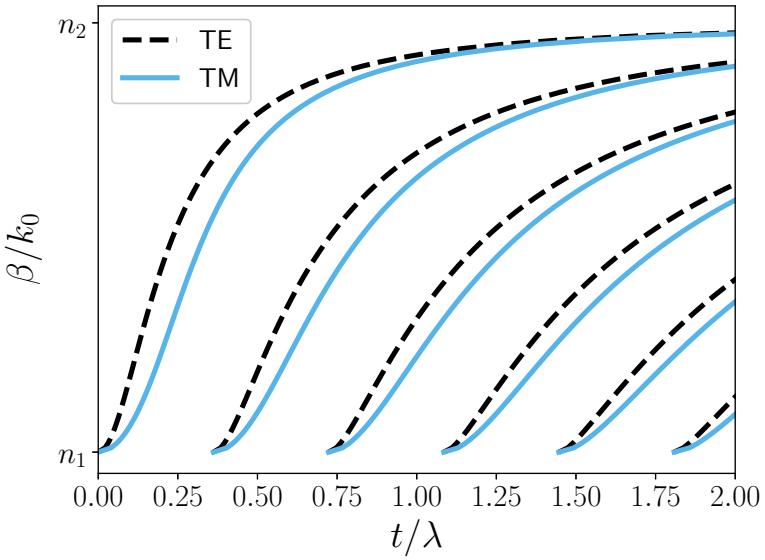

Figure 2.3: A dispersion plot showing the allowed TE and TM modes for a symmetric planar waveguide as shown in 2.2.

The dispersion relation becomes important when we want to design waveguides that can operate over multiple frequencies. In Chapter 3 the dispersion in the waveguide will play a role in how nonlinear effects emerge.

Although analytical solutions exist for planar dielectric waveguides, once we encase the side of the core and deal with non-planar waveguide analytical solutions generally do not exists and we are left with numerical simulation to ascertain the modes. How the mode confinement in an embedded waveguide can appear is illustrated in Figure 2.4. Techniques for how we will do this numerically will be treated in Chapter 4.

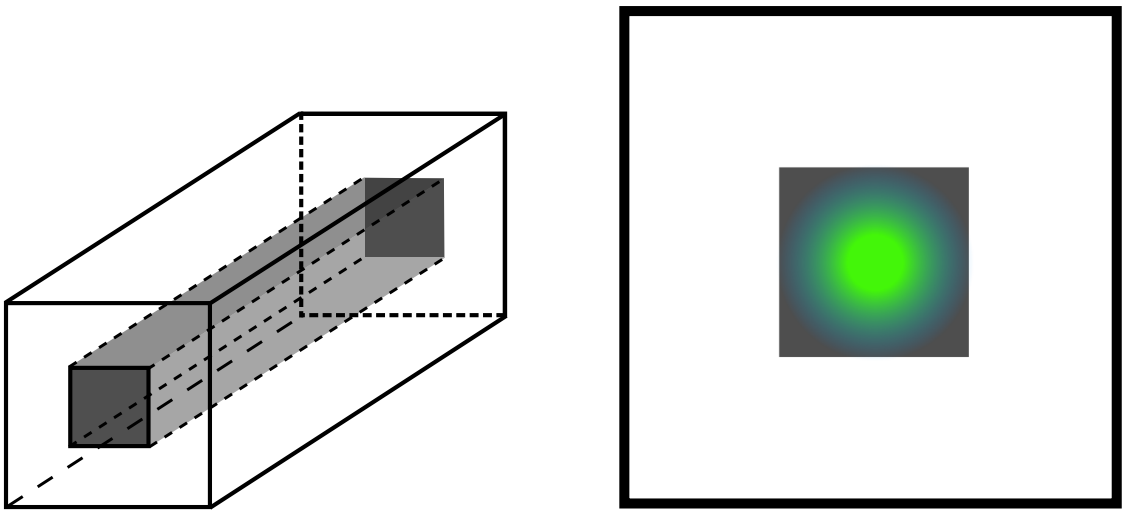

(a) (b)

Figure 2.4: Depiction of the fundamental mode in an embedded waveguide. To the left in Figure 2.4a we have a schematic waveguide with a centre core surrounded by cladding. To the right in Figure 2.4b we see an illustration of the confinement of a fundamental mode.

2.3 Bloch waves and periodic structures

We often find ourselves in a situation where we have a need to look at periodic structures. Though much of the research stem from being able to predict the behaviour of periodic homogeneous materials, such as crystals, the same results can be used for bigger structures where we design patterning of materials with a given periodicity. It is highly convenient to design materials like this since we then can analyse and categorise a smaller segment or unit cell, simplifying the problem and enabling analysis of devices that would be to large to simulate. When we are working with nanophotonic systems, the size of the systems we want to design quickly becomes unfeasible to simulate or treat without being able to treat the system as a homogeneous or periodic structure. This is because when we are interested in the macroscopic behaviour of a photonic structure, and we do not have a way to simplify the problem, we need to simulate big structures but with a very fine spatial resolution. We might need to resolve structures on nano or micrometer scale but the overall structure can be on meter scale. This type of simulations are usually unfeasible and in the best case very slow and costly, which is why everything greatly simplifies if we can use techniques like periodicity to perform calculation on a small part of the structure. Readers interested in wave propagation in different kinds of photonic structures are advised to read Markos and Soukoulis [17]. Knowledge of periodic crystal structures can also be found in solid-state physics books like [18] [19].

Let us look at the periodic structure of a waveguide depicted in Figure 2.5.
In order for us to take advantage of periodicity we want to design the system such that

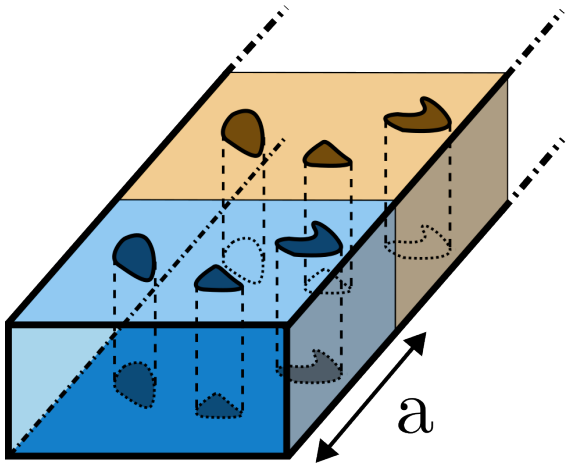

Figure 2.5: Example of a periodic patterned waveguide structure where the structure repeats after a distance a. The unit cell is coloured differently for easier distinction.

the incoming and outgoing waves are equal, save for a phase rotation, as expressed in Equation (2.4)

$$\psi_k(\mathbf{r} + \mathbf{a}) = e^{i\mathbf{k}\cdot\mathbf{a}}\psi_k(\mathbf{r}) \tag{2.4}$$

where $\mathbf{a}$ denotes the length of the periodic unit cell. Waves that behave like this are called Bloch waves, so named after Bloch who coined the requirement in 1929 [20] [18] [21]. An understanding of the concept of Bloch periodic structures will become relevant when we want to tailor waveguides by changing the geometry through patterning.

3

Nonlinear optics

In this chapter, we present the theory of nonlinear optics. We start with a basic description of what kind of nonlinearity we refer to with nonlinear optics. Thereafter we progress into the theory needed for us to understand the concept of optical parametric amplification (OPA). To reach this goal, we will treat nonlinear effects of materials and how these combined effects can be used to understand the intermodulation phenomenon four-wave mixing (FWM), which is used to describe the concept of OPA. Readers on the hunt for general books on the subject of nonlinear optics are advised to read the books (all named "Nonlinear optics") by Moloney and Newell [22], Robert Boyd [23], and Nicolaas Bloembergen [24]. I can also recommend the video series by the International School on Parametric Nonlinear Optics (ISPNLO) held in 2015 [25].

3.1 Nonlinear effects in materials

With the term "nonlinear optics" we refer to effects that stem from the permittivity and permeability of a material depending on the field strength:

$$\begin{aligned} \mathbf{D} &= \varepsilon(\mathbf{E})\mathbf{E} \\ \mathbf{B} &= \mu(\mathbf{H})\mathbf{H} \end{aligned} \tag{3.1}$$

From here we will focus on the electric field. Recall that we can express the displacement field as the electric field in free space plus a polarisation term:

$$\mathbf{D} = \varepsilon(\mathbf{E})\mathbf{E} = \varepsilon_0\mathbf{E} + \varepsilon_0\chi\mathbf{E}. \tag{3.2}$$

We then express the polarisation as a power series expansion, starting with scalar notation to simplify the introduction:

$$P = \varepsilon_0 \left[\chi^{(1)} E + \chi^{(2)} E^2 + \chi^{(3)} E^3 + ... \right] \\ = P^{(1)} + P^{(2)} + P^{(3)} + ... \tag{3.3}$$

From Equation (3.3), we see that the nonlinear dependence emerge from the higher-orders in the expansion. $\chi^{(1)}$ is our normal linear susceptibility that we will recognise from Equation (2.3), while $\chi^{(2)}$ and $\chi^{(3)}$ are the second- and third-order susceptibilities etc. From the expansion we see that higher-orders are more sensitive to field strength and the scale of the higher-order contributions to the polarisation depend on the susceptibilities.

Let us put some order of magnitude on these constants so we can get a feeling of how they affect the fields. We can estimate these values by calculating the characteristic atomic field strength $E_{at} = e/(4\pi\varepsilon_0 a_0^2)$, where e is the elementary charge and $a_0 = 4\pi\varepsilon_0\hbar^2/(me^2)$ is the Bohr radius of hydrogen and m is the electron mass. Plugging in values gives us $E_{at} = 5.14 \times 10^{11}$ V/m. The first-order susceptibility, $\chi^{(1)}$, is of the order of unity for condensed matter, and we can estimate the orders of $\chi^{(2)}$ and $\chi^{(3)}$ with $\chi^{(1)}/E_{at}$ and $\chi^{(1)}/E_{at}^2$, respectively [23]. The orders of magnitude are presented in table 3.1.

Table 3.1: Table showing order of magnitude for the first three orders of suceptibilities[23].

Suceptibility $\chi^{(n)}$	Typical order of magnitude
$\chi^{(1)}$	10^0
$\chi^{(2)}$	10^{-12} m/V
$\chi^{(3)}$	10^{-24} m^2/V^2

From table 3.1 and Equation (3.3) we can deduce that for these effects to appear clearly we need to either have large field strengths or letting the light pass through large volumes of material, so it can accumulate enough nonlinear phase.

Before we go into a more thorough description of the nonlinear effects, it is worth pointing out that what we are talking about here is electronic polarisation, effects induced on the electrons in the materials under the influence of an electric field. In fact, the nonlinear effects in materials can be caused by different physical mechanisms, as summarised by Boyd [23] and presented in table 3.2. The focus of this thesis is on electronic polarisation, sometimes referred to as instantaneous polarisation due to its short response time, but there are other nonlinear effects that operate on longer time scales. The extremes being heating effects in materials that have response times on the order of milliseconds.

Moving back to electronic polarisation, we can describe the general polarisation field as a combination of multiple electric fields, each with its own frequency, which may or

Table 3.2: Values of the nonlinear refractive index for linear polarised light [23]. The response time is the time it takes to reach the steady state after we 'turn on our laser'.

Nonlinear mechanism	n_2 [cm^2/W]	$\chi^{(3)}$[m^2/V^2]	Response time [s]
Electronic polarisation	10^{-16}	10^{-22}	10^{-15}
Molecular orientation	10^{-14}	10^{-20}	10^{-12}
Electrostriction	10^{-14}	10^{-20}	10^{-9}
Saturated atomic absorption	10^{-10}	10^{-16}	10^{-8}
Thermal effects	10^{-6}	10^{-12}	10^{-3}

may not be the same,

$$\mathbf{P} = \varepsilon_0 \left[\chi^{(1)}\mathbf{E}_1 + \chi^{(2)}\mathbf{E}_1\mathbf{E}_2 + \chi^{(3)}\mathbf{E}_1\mathbf{E}_2\mathbf{E}_3 + ... \right], \tag{3.4}$$

which opens up for intermodulation and interaction between different frequencies.

To understand this intermodulation, we need to start from the time dependent expression for the linear polarisation field where the polarisation is expressed as a convolution of the time-dependent susceptibility and the time-dependent electric field.

$$\mathbf{P}(t) = \varepsilon_0 \int_{-\infty}^{\infty} \chi(t-\tau)\mathbf{E}(\tau)d\tau. \tag{3.5}$$

From causality we require that $\chi(t-\tau) = 0$ for $\tau < t$, and since complex values of χ are nonphysical, the reality conditions require χ to be real [26]. For higher-orders, the susceptibility becomes a tensor and similarly to the expression in Equation (3.5), we can express the polarisation in Equation (3.4) for its j:th component as:

$$\begin{aligned} P_j(t) = {} & \varepsilon_0 \int_{-\infty}^{\infty} \chi^{(1)}_{jk}(t-\tau_1)E_k(\tau_1)d\tau_1 \\ & + \varepsilon_0 \int_{-\infty}^{\infty}\int_{-\infty}^{\infty} \chi^{(2)}_{jkl}(t-\tau_1, t-\tau_2)E_k(\tau_1)E_l(\tau_2)d\tau_1 d\tau_2 \\ & + \varepsilon_0 \int_{-\infty}^{\infty}\int_{-\infty}^{\infty}\int_{-\infty}^{\infty} \chi^{(3)}_{jklm}(t-\tau_1, t-\tau_2, t-\tau_3)\hat{E}_k(\tau_1)\hat{E}_l(\tau_2)\hat{E}_m(\tau_3)d\tau_1 d\tau_2 d\tau_3 \\ & + ... \end{aligned} \tag{3.6}$$

where we are using the Einstein summation convention [27] for summing over indices. This expression may seem a bit tumbling at start, but some interesting things happen when we view this expression in the frequency domain. Before presenting this expression, recall that the exponential representation of a Dirac delta function δ can be written as [28, 29]

$$\delta(x - x_0) = \frac{1}{2\pi}\int_{-\infty}^{\infty} e^{ik(x-x_0)}dk. \tag{3.7}$$

With this, we can express the polarisation by Fourier transforming Equation (3.6) yielding

$$\begin{aligned}\hat{P}_j(\omega) = \varepsilon_0 \hat{\chi}^{(1)}_{jk}(\omega)\hat{E}_k \\ + \frac{\varepsilon_0}{2\pi}\iint_{-\infty}^{\infty} \hat{\chi}^{(2)}_{jkl}(\omega_1,\omega_2)\hat{E}_k(\omega_1)\hat{E}_l(\omega_2)\delta(\omega_1+\omega_2-\omega)d\omega_1 d\omega_2 \\ + \frac{\varepsilon_0}{(2\pi)^2}\iiint_{-\infty}^{\infty} \hat{\chi}^{(3)}_{jklm}(\omega_1,\omega_2,\omega_3)\hat{E}_k(\omega_1)\hat{E}_l(\omega_2)\hat{E}_m(\omega_3)\delta(\omega_1+\omega_2+\omega_3-\omega)d\omega_1 d\omega_2 d\omega_3 \\ + ... \\ .\end{aligned} \tag{3.8}$$

From the expression in Equation (3.8) we can deduce that we have requirements on the frequencies to match for second -and higher-order effects from the delta functions. For example for third-order susceptibilities we have the requirement that

$$\omega_1 + \omega_2 + \omega_3 - \omega = 0, \tag{3.9}$$

for the effects to appear. This is something that we will use in the context of FWM, which we will treat in Section 3.2. We can also deduce multiple symmetry requirements of the tensors which is very useful since $\chi^{(3)}$, for example, has 3^4 different elements. For details regarding symmetry derivations, see, for instance, Refs [26] [23].

3.2 Four wave mixing

From Equation (3.8) in Section 3.1, we could see that we had requirements on the frequencies. For the third-order process we have 4 different frequencies that needs to obey Equation (3.9). The interaction between these four frequencies are what is called four wave mixing. If we assume we have a material where we can express the susceptibility as a scalar quantity we can write out all the possible complex amplitudes for third-order nonlinear interactions. This will help with the intuition of the effects. Negative frequencies are allowed and we interpret them as the complex conjugate of the field. We end up with the following expressions where we combine all possible combinations that result in a polarisation contribution at one frequency [23]:

$$\begin{aligned} P(\omega_1) &= \varepsilon_0\chi^{(3)}\left(3E_1E_1^* + 6E_2E_2^* + 3E_3E_3^*\right)E_1, & P(3\omega_1) &= \varepsilon_0\chi^{(3)}E_1^3, \\ P(\omega_2) &= \varepsilon_0\chi^{(3)}\left(6E_1E_1^* + 3E_2E_2^* + 3E_3E_3^*\right)E_2, & P(3\omega_2) &= \varepsilon_0\chi^{(3)}E_2^3, \\ P(\omega_3) &= \varepsilon_0\chi^{(3)}\left(6E_1E_1^* + 6E_2E_2^* + 3E_3E_3^*\right)E_3, & P(3\omega_3) &= \varepsilon_0\chi^{(3)}E_3^3, \end{aligned}$$

$$
\begin{aligned}
P(\omega_1+\omega_2+\omega_3) &= 6\varepsilon_0\chi^{(3)}E_1E_2E_3, & P(\omega_1+\omega_2-\omega_3) &= 6\varepsilon_0\chi^{(3)}E_1E_2E_3^*,\\
P(\omega_1-\omega_2+\omega_3) &= 6\varepsilon_0\chi^{(3)}E_1E_2^*E_3, & P(-\omega_1+\omega_2+\omega_3) &= 6\varepsilon_0\chi^{(3)}E_1^*E_2E_3,
\end{aligned}
$$

$$
\begin{aligned}
P(2\omega_1+\omega_2) &= 3\varepsilon_0\chi^{(3)}E_1^2E_2, & P(2\omega_1+\omega_3) &= 3\varepsilon_0\chi^{(3)}E_1^2E_3,\\
P(2\omega_2+\omega_1) &= 3\varepsilon_0\chi^{(3)}E_2^2E_1, & P(2\omega_2+\omega_3) &= 3\varepsilon_0\chi^{(3)}E_2^2E_3,\\
P(2\omega_3+\omega_1) &= 3\varepsilon_0\chi^{(3)}E_3^2E_1, & P(2\omega_3+\omega_2) &= 3\varepsilon_0\chi^{(3)}E_3^2E_2,\\
P(2\omega_1-\omega_2) &= 3\varepsilon_0\chi^{(3)}E_1^2E_2^*, & P(2\omega_1-\omega_3) &= 3\varepsilon_0\chi^{(3)}E_1^2E_3^*,\\
P(2\omega_2-\omega_1) &= 3\varepsilon_0\chi^{(3)}E_2^2E_1^*, & P(2\omega_2-\omega_3) &= 3\varepsilon_0\chi^{(3)}E_2^2E_3^*,\\
P(2\omega_3-\omega_1) &= 3\varepsilon_0\chi^{(3)}E_3^2E_1^*, & P(2\omega_3-\omega_2) &= 3\varepsilon_0\chi^{(3)}E_3^2E_2^*.
\end{aligned}
\tag{3.10}
$$

So how do we interpret this? What we see is a manifestation of a parametric process that can be described by an energy diagram presented in figure 3.1. Here the initial and final energy states are the same, so if we have two photons with frequency ω_1 and ω_2 entering the system, they can briefly excite a virtual energy level. Conservation of energy means that when the energy state relaxes, the energy needs to radiate out again. The result is a combination of photons that contains the same total energy going in and out of the system, forming a parametric process.

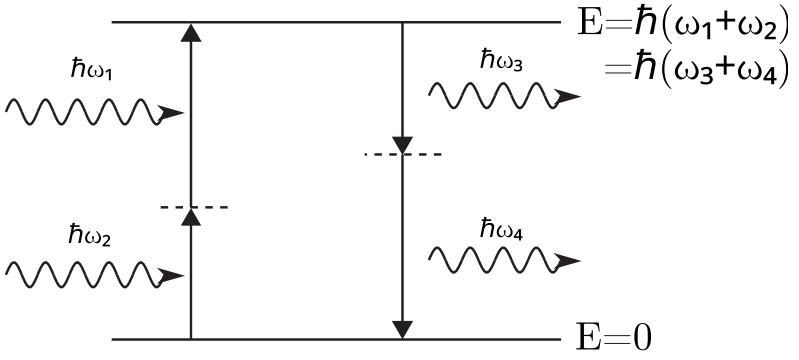

Figure 3.1: Energy levels of a four wave mixing process. The energy of the incoming photons (ω_1 & ω_2) adds up to a virtual energy level that later relaxes into two new photons with different frequencies (ω_3 & ω_4).

Let us, for instance, take the first term in the expression for $P(\omega_1)$ in Equation (3.10). The only way for the system to produce a photon with frequency ω_1 is to excite the energy state with energy from ω_1 and then add another frequency that comes back during the relaxation. This would result in a situation where the photons interacting in figure 3.1 would obey $\omega_2 = \omega_3$ and $\omega_1 = \omega_4$.

A similar argument can be made for second-order effects and we would then end up with another set of relations like in Equation (3.10) but instead the four frequencies we

treat here we would have three different frequencies. For details, see for example Ref. [23].

The idea of mixing different frequencies in a nonlinear material was known early on but the field of nonlinear optics really took off in the 1960s when Franken, Hill, Peters and Weinreich experimentally demonstrated the generation of optical harmonics in 1961 [30]. They used second-order nonlinearity to generate a harmonic of a pump frequency, where two photons of frequency ω are converted into one photon with frequency 2ω, so-called second harmonic generation (SHG). The same year Kaiser and Garett also experimentally showed the nonlinear optical phenomenon "two photon absorption" in CaF_2 [31] where 2 photons through a virtual energy level could reach a higher energy state in the material and produce a higher frequency photon. The theory of this operation was already put forth by Göppert-Mayer in 1931 [32], but it took 30 years before it could be measured. Once SHG was demonstrated, the concept of third harmonic generation (THG) was quickly demonstrated. In THG, we combine three photons to create one photon with thrice the frequency, 3ω, through a third-order nonlinear process. This was demonstrated in 1962 by Terhune, Maker and Savage [33]. The same year, Bloembergen, Armstrong, Ducuing, and Pershan used quantum mechanical perturbation theory to first theoretically describe the process that Franken et al. had demonstrated in 1961 [34].

3.2.1 Phase matching

We saw in the previous section that we got a requirement on energy conservation for the FWM to work, that resulted in a relation between frequencies in the mixing. We also have another requirement on the waves, with different frequencies, that interact and that is what is called phase matching. This means that for the waves to interact and properly mix they need to be close in phase.
For a four wave mixing process, like in figure 3.1 we have a phase matching condition of

$$\Delta\beta = (\beta_1 + \beta_2 - \beta_3 - \beta_4)\,. \tag{3.11}$$

Ideally the mismatch should be zero, which in turn would mean that we have conservation of momentum for the photons. There are different ways to handle this depending on material properties. Midwinter and Warner defined two types of phase matching for second-order processes for bifringent materials in 1962 [35]. Here we use the crystal orientation to give different dispersion for different frequencies to counteract unwanted dispersion. Another approach to phase matching is to change the propagation constant by changing the angle of which the beams enter the material, as demonstrated by Hobden [36]. The above approaches uses slabs of materials but we can also achieve phase matching over a periodic structure. This approach was originally proposed by Bloembergen, Armstrong, Ducuing, and Pershan in 1962 [34] and is named quasi-phase matching (QPM). The use of QPM has many applications and opens up many possibilities in combination with better materials engineering [37][38]. For a review of different

quasi-matched materials, see for instance Ref. [39]. The idea is that one engineers the dispersion of the material so that at the end of each periodic segment the phase mismatch is negated. For this approach to work efficiently, the length of these unit cells in the periodic structure needs to be sufficiently smaller than the coherence length L_C

$$L_C = \frac{\pi}{\Delta k}. \tag{3.12}$$

We can tailor the QPM over longer distances than L_c but at the expense of weaker nonlinear interaction. This can be relevant in situations where it is hard to manufacture the material thin enough and we can then simplify the manufacturing at the expense of weaker nonlinear interaction per distance. Another reason might be that we have unwanted nonlinear processes with other frequency components that we want to remove, then we can design the material such that phase matching for the unwanted process in unfavourable. The process of manufacturing these periodic materials often results in distributed noise that covers a wide frequency spectrum where basically everything is a little bit phase matched due to manufacturing tolerances [40]. A good resource for QPM tuning is Fejer and Byer [41]. If one wants to utilise FWM using pulsed waves, the phase matching with first-order dispersion is usually not enough – we also need to take the higher-order dispersion, like group velocity into account, but if we are operating in a continuous wave (CW) or quasi-CW regime, these effects can often be neglected [42].

3.3 Optical parametric amplifiers

In practical terms, we can use the concept of FMW described in Section 3.2 to amplify a desired signal, by means of difference frequency generation, also called optical parametric amplification (OPA). What we want is to use the energy of a pump laser and transfer it to a desired signal. To achieve this, we need to ensure that when the excited state, as described in figure 3.1, decomposes into two different photons we want to tailor it so that one of the exited photons has the frequency of the signal. The way to handle this most easily is to ensure that the mixing allows the pump to interact with itself to form a higher energy state and then relax down into the signal frequency. This in turn means that the frequency of the signal must be lower than twice the frequency of the pump. As a result of the mixing process, we will also have another photon from the relaxation that has a frequency separate from the pump and signal. This is called an idler frequency. The concept of OPA is depicted in figure 3.2.

The effect of OPA was first measured by Harris, Oshman and Byer in 1967 [43], but the optical effect was treated theoretically by Siegman, Yariv and Louisell earlier in 1961 [44]. The OPA has an advantage regarding its amplification, compared to other techniques, due to the fact that it has very low noise [44][45]. The downside of the OPA, as we have seen from expression of $\chi^{(3)}$, is that the interaction is very weak, and we therefore need

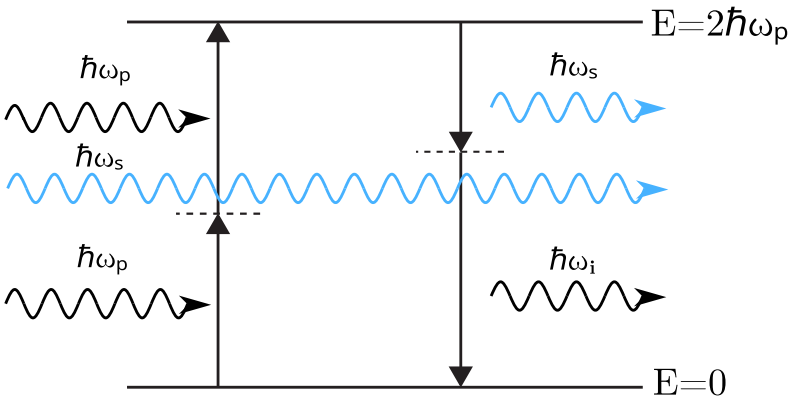

Figure 3.2: Energy levels for a four wave mixing process in a optical parametric amplifier. two photons of the pump laser, with frequency ω_p, form an energy state that relaxes into two photons for the signal (ω_s) and idler (ω_i) frequency. The signal photon amplifies the existing signal photons that passes through the system, indicated in blue.

to propagate the light through large volumes of material to accumulate phase. Since the light needs to interact with large volume it also attenuates due to losses in the material. For amplification to occur we therefore must ensure that the losses in the material is low enough so it doesn't negate the amplification.

4 Electromagnetic simulations

In this chapter, I will go through the different types of numerical methods that we need to achieve our goals, presented in Chapter 1, of simulating arbitrary patterned Bloch periodic waveguides using the theory described in Chapters 2 and 3. The chapters will describe the use of nonlinear Schrödinger equations to simulate the propagation over long distances and how we will use finite element methods to determine the constants that we need in the nonlinear Schrödinger equations. For a good overall view of numerical methods in the field of photonics, see for instance Obayya [46].

4.1 Simulate the propagation of optical signals in waveguides

In this section, we will treat the method by which we simulated wave propagation over longer distances. When we are after results of wave propagation over long photonic structures spanning up to meters in length, as used in Ref. [1], full-wave simulations of the entire waveguide structure becomes computationally infeasible without some simplification as mentioned in the beginning of Chapter 4. In the following sections in this chapter, we will introduce how this can be done by solving a nonlinear Schrödinger equation (NLSE) to get an expression for how the excited wave propagates along the longitudinal direction of the waveguide.

4.1.1 Nonlinear Schrödinger equation

We will here go through the steps taken in order to arrive at the NLSE that we will use to calculate the wave propagation. As the name suggest, it is a extended variation of the Schrödinger equation, first published by Erwin Schrödinger i 1926 [47]. The NLSE was

first written down in 1962 by Towes, Garmire and Chiao [48], but is in itself a simplification of the Ginzburg-Landau equation first published in 1959 by Landau and Ginzberg [49][50]. For further details of the derivations we refer to the work by Marhic [51] and Agrawal [42]. The derivation will be made with just linear components and the nonlinear contributions will be added afterwards as a perturbation. In Section 2.1 we discussed the concept of dispersion and it will, here, play a big role in setting up the NLSE. For the problems we are interested in, we want to address a range of frequencies, ω, for the solution to work we need them centred round a centre frequency, ω_c and that the difference

$$\Omega = \omega - \omega_c \tag{4.1}$$

to be sufficiently small. We can the express the dispersion as a power series:

$$\beta(\omega) = \beta(\omega_c + \Omega) = \beta_c + \sum_{n=1}^{\infty} \frac{\beta^{(n)}}{n!}\Omega^n. \tag{4.2}$$

where

$$\beta_c = \beta(\omega_c) \quad \text{and} \quad \beta^{(n)} = \left.\frac{d^n\beta}{d\omega^n}\right|_{\omega=\omega_c}. \tag{4.3}$$

We express the electric field along the longitudinal direction, $\hat{z}$, with the slowly varying envelope $\mathbf{A}(z,t)$.

$$\mathbf{E}(z,t) = \frac{1}{2}\left[\mathbf{A}(z,t)e^{i(\beta_c z - \omega_c t)} + c.c.\right] \tag{4.4}$$

where *c.c.* stands for the complex conjugate of the field. This is an assumption that E varies slowly over time and that most change occurs in the propagation direction.

In order to reach the final expression we will first decompose $\mathbf{A}$ in terms of its Fourier decomposition, $\mathbf{B}(\Omega)$. Then we will differentiate and compare expressions taking derivatives and compare expressions to obtain our results.

At the start we have our envelope

$$\mathbf{A}(0,t) = \int_{-\infty}^{\infty} \mathbf{B}(\Omega)e^{-i\Omega t}d\Omega \tag{4.5}$$

Since we assume linear propagation along the longitudinal direction we can describe the envelope at any position along the propagation axis as

$$\mathbf{A}(z,t) = \int_{-\infty}^{\infty} \mathbf{B}(\Omega)e^{i(\beta-\beta_c)z - i\Omega t}d\Omega. \tag{4.6}$$

We then take the derivative of Equation (4.6), which yields

$$\frac{\partial\mathbf{A}(z,t)}{\partial z} = \int_{-\infty}^{\infty} \mathbf{B}(\Omega)i(\beta-\beta_c)e^{i(\beta-\beta_c)z - i\Omega t}d\Omega. \tag{4.7}$$

From Equation (4.2) we know that we can replace the parts containing $\beta - \beta_c$ and we get

$$\frac{\partial \mathbf{A}(z,t)}{\partial z} = i \int_{-\infty}^{\infty} \mathbf{B}(\Omega) \left(\sum_{n=1}^{\infty} \frac{\beta^{(n)}}{n!} \Omega^n \right) e^{i(\beta-\beta_c)z - i\Omega t} d\Omega \tag{4.8}$$

If we then where to take the m:th derivative of (4.6) with respect to t, we get

$$\frac{\partial^m \mathbf{A}(z,t)}{\partial t^m} = \int_{-\infty}^{\infty} \mathbf{B}(\Omega)(-i\Omega)^m e^{i(\beta-\beta_c)z - i\Omega t} d\Omega. \tag{4.9}$$

Comparing Equations (4.9) and (4.8) we note that we can replace the integral in Equation (4.8) with a sum of time derivatives which results in

$$\frac{\partial \mathbf{A}(\mathbf{z},\mathbf{t})}{\partial z} - \sum_{n=1}^{\infty} \frac{i^{n+1}\beta^{(n)}}{n!} \frac{\partial^n \mathbf{A}(\mathbf{z},\mathbf{t})}{\partial t^n} = 0, \tag{4.10}$$

which is our expression for the wave propagation taking only dispersion into account. To reach our final expression we need to add the loss of the propagation constant, α and the nonlinear part. The loss is incorporated by adding the term $\alpha/2$ to the dispersion. The nonlinear effect is added using a nonlinear parameter γ to achieve the full non-linear Schrödinger equation

$$\frac{\partial \mathbf{A}(\mathbf{z},\mathbf{t})}{\partial z} + \frac{\alpha}{2} - \sum_{n=1}^{\infty} \frac{i^{n+1}\beta^{(n)}}{n!} \frac{\partial^n \mathbf{A}(\mathbf{z},\mathbf{t})}{\partial t^n} = i\gamma |\mathbf{A}(z,t)|^2 \mathbf{A}(z,t). \tag{4.11}$$

When we are operating in a regime where the frequency components are close together we can assume that the nonlinear part has a constant frequency dependence and if we in turn have a system where the nonlinearity has a low spacial dependency we can simplify the expression of γ to be

$$\gamma = \frac{2\mu_0 \omega \chi^{(3)}}{8\overline{n}^2 A_{eff}}, \tag{4.12}$$

where $\overline{n}$ is the effective refractive index and the effective area, A_{eff}, is a measure on the transverse mode profile overlap [42]:

$$A_{eff} = \frac{\left[\iint (\psi^* \psi) dxdy\right]^2}{\iint (\psi^* \psi)^2 dxdy}. \tag{4.13}$$

Here ψ denote the transverse component of the electric field, with depending on x and y. What Equation (4.12) and (4.13) describe is that we can get a nonlinear effect either by choosing a material with high $\chi^{(3)}$ or by ensuring that the field concentrates in the cross

area as much as possible. To be able to achieve stable solutions for the NLSE, so called solitons, requires us to either tailor the spatial details of our system or tweak the time dependence, like sending pulses of light. The first soliton solution achieved was a spatial soliton, realised by Garmire, Chiao and Townes in 1964 [52] and the first temporal soliton solution using pulses of light was realised in optical fibers by Tappert and Hasegawa in 1973 [53].

4.1.2 Split-step Fourier method

In order to solve the NLSE for the wave propagation, described in Section 4.1.1, we can use the split-step Fourier method (SSFM) first developed by Tappert in 1972 at Bell Laboratories [54]. The method is based on that we separate the components of the NLSE (4.11) into a linear and nonlinear part and then assume that they can act separately on the wave function during small steps in the longitudinal direction. To speed this up one then lets the linear part act in the frequency domain and the nonlinear part in the time domain. The process goes as follows [42]:

We take Equation (4.11) and express it like

$$\frac{\partial \mathbf{A}(z,t)}{\partial z} = \left[-\frac{\alpha}{2} + \sum_{n=1}^{\infty} \frac{i^{n+1}\beta^{(n)}}{n!} \frac{\partial^n}{\partial t^n} + i\gamma |\mathbf{A}(z,t)|^2 \right] \mathbf{A}(\mathbf{z},\mathbf{t}) = \left[\hat{D} + \hat{N} \right] \mathbf{A}(z,t) \tag{4.14}$$

where $\hat{D}$ expresses an operation representing the linear part of the NLSE, while $\hat{N}$ represent the nonlinear part. If we then take a small enough step, h, in the longitudinal z direction, we assume that the numerical error induced by separating $\hat{D}$ and $\hat{N}$ is small. This means that we can write the solution for propagation of a small step, h, as

$$A(z+h,t) \approx e^{h\hat{D}} e^{h\hat{N}} A(z,t) \tag{4.15}$$

We then note from Equation (4.14) that the linear part $\hat{D}$ contains all the time derivatives. These are cumbersome to calculate, but we note that the time derivatives become much more simple to calculate in the frequency domain

$$\mathscr{F}\left\{\hat{D}\right\} = \mathscr{F}\left\{ -\frac{\alpha}{2} + \sum_{n=1}^{\infty} \frac{i^{n+1}\beta^{(n)}}{n!} \frac{\partial^n}{\partial t^n} \right\} = -\frac{\alpha}{2} + \sum_{n=1}^{\infty} \frac{i^{n+1}\beta^{(n)}}{n!} (i\omega)^n, \tag{4.16}$$

where $\mathscr{F}$ denotes the Fourier transform and the transform gives $(i\omega)$ in place of the time derivatives. Thus, the easiest way to calculate is to propagate the linear part in the frequency domain and the nonlinear part in the time domain.

Putting it together we then get the expression for one spatial step, h, to be

$$A(z+h,t) = \mathscr{F}^{-1}\left\{ e^{h\mathscr{F}\{\hat{D}\}} \mathscr{F}\left\{ e^{h\hat{N}} A(z,t) \right\} \right\}, \tag{4.17}$$

which has an accuracy to the second-order in the step size h [42].

We can further increase the accuracy of the SSFM by using a staggered step where the nonlinear part is allowed to act on A at the midpoint between steps, $h/2$. This is known as the symmetrized split-step Fourier method, illustrated in Figure 4.1, first used by Feit, Fleck, and Morris in 1976 [55].

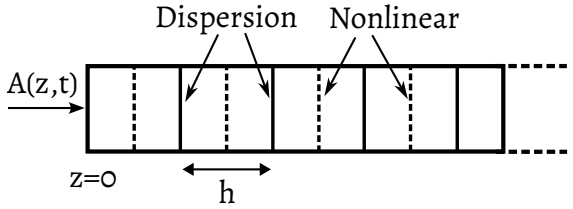

Figure 4.1: Illustration of symmetrized split-step Fourier method, showing the placement in the geometry when dispersion and nonlinearity are added.

The symmetrized SSFM instead expresses Equation (4.15) as two half step linear propagation on the boundaries and one full nonlinear step in the segment

$$A(z+h,t) \approx e^{\frac{h}{2}\hat{D}} exp\left(\int_z^{z+h} \hat{N}(z')dz'\right) e^{\frac{h}{2}\hat{D}} A(z,t). \tag{4.18}$$

When we use a small step size the integral in (4.18) can be approximated with

$$exp\left(\int_z^{z+h} \hat{N}(z')dz'\right) \approx e^{h\hat{N}}. \tag{4.19}$$

We can then use a trick to speed up the calculations. By combining Equations (4.19) and 4.18 we can rewrite them as

$$A(z+h,t) \approx e^{\frac{h}{2}\hat{D}} e^{h\hat{N}} e^{\frac{h}{2}\hat{D}} A(z,t) = e^{-\frac{h}{2}\hat{D}} \left(e^{h\hat{D}} e^{h\hat{N}}\right) e^{\frac{h}{2}\hat{D}} A(z,t). \tag{4.20}$$

From Equation (4.20) we note that the middle section contains a full step length. This means that for the propagation over a longer length containing M steps we can write the final expression of A

$$A(z+Mh,t) \approx e^{-\frac{h}{2}\hat{D}} \left(\prod_{m=1}^{M} e^{h\hat{D}} e^{h\hat{N}}\right) e^{\frac{h}{2}\hat{D}} A(z,t). \tag{4.21}$$

This means that apart from the beginning and end we can evaluate the linear and nonlinear contribution with the same step length, cutting the number of Fourier transforms down by almost a factor of 2 [42].

4.2 Determining propagation and dispersion constants

This section will describe the use of the finite element method to determine the dispersion for a Bloch periodic waveguide. We will introduce the finite element method and how we can use it to solve for loss and dispersion by the use of eigenmode simulations. The purpose of this section is to present the tools needed to simulate these waveguide and provide an understanding of what different steps in the process do, while providing references for further reading on the subject.

4.2.1 Finite element method

Since it was first conceived in 1943 by Courant [56], the finite element method (FEM) has grown to be a very popular and useful numerical tool to solve partial differential equations (PDE) over some geometry. The method works by subdividing the geometry into smaller mesh cells and approximate the solution with a finite number of parameters, referred to as degrees of freedom (DOF). The process of subdividing the geometry is called meshing, where we partition the geometry with a mesh consisting of polygons and polyhedrons. The physics calculations are then performed on these elements and the size of the elements determine how accurately the physics can be described. A good reference on the use of FEM in electromagnetism is [57]. This thesis will not go into details of the exact workings of the finite element method, but will treat subjects needed to understand and use FEM for solving for the dispersion in optical waveguides. For a thorough understanding of finite element solvers, read for example Ottosen and Petersson ,[58], but also manuals from commercial FEM packages usually have a good explanation, see for example COMSOL [59–61].

Having many elements results in more calculations to be performed since we need to determine more degrees of freedoms (DOF). It is always of interest to keep the DOF down, both to cut down the simulation times down and also to be able to utilise available memory better. In paper I [62], we presented a meshing strategy based on a posteriori information of the calculated electric fields on the domain, implemented in COMSOL [63]. By starting with a course mesh and then refining mesh elements that exhibit larger errors, we can ensure that we only refine elements that needs refining to resolve the electromagnetic behaviour, as demonstrated in Figure 4.2.

In the following subsections, we will go through how we express the strong form of the PDE of our problem into the weak form (Section 4.2.1.1), how we deal with different boundaries for our simulation domain (Section 4.2.2) and how we rewrite our electromagnetic expression in order to solve for for eigenmodes at a specified frequency (Section 4.2.3).

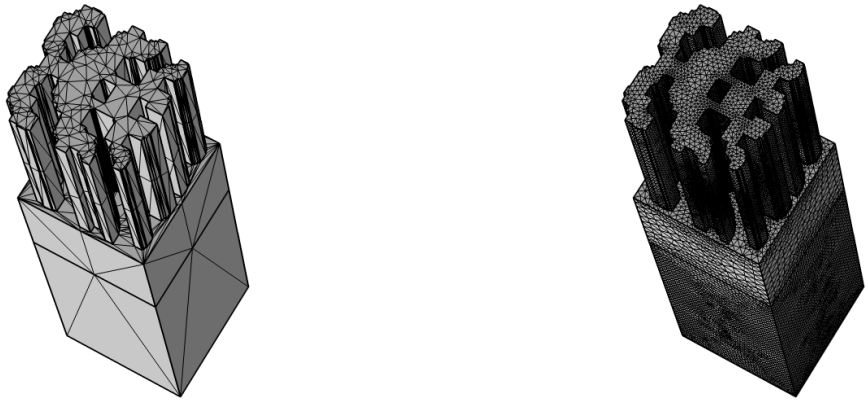

(a) (b)

Figure 4.2: Demonstration of a mesh refinement in a 3D structure were regions with smaller features are resolved with a denser mesh because of the need to resolve the electromagnetic fields.

4.2.1.1 Weak expression

When solving for a physics based PDE with FEM, we do not need to use the original form of the PDE, called the strong form. Instead, we express the variational form of the PDE, called the weak form.

The concept revolves around expressing the original PDE as an integral equation. The solutions of interest are then approximated with a set of basis functions on small sections of the integral. We then multiply the original PDE expression with a test function, this test function can then be tweaked and chosen in a way that we over the integrated area can approximate the value of our solution. This approximation can then be computed on smaller element section of the total volume.

To arrive at the weak expression needed to solve for the electric field, we start with the wave equation for the electric field:

$$\nabla \times \left(\frac{1}{\mu} \nabla \times \mathbf{E} \right) - \varepsilon \frac{\omega^2}{c^2} \mathbf{E} = 0. \tag{4.22}$$

We then get the weak formulation by multiplying the expression in Equation (4.22) with a test function, $\mathbf{v}$, to yield:

$$F_E(\mathbf{v}, \mathbf{E}) = (\nabla \times \mathbf{v}) \cdot \frac{1}{\mu} (\nabla \times \mathbf{E}) - \varepsilon \frac{\omega^2}{c^2} \mathbf{v} \cdot \mathbf{E} = 0. \tag{4.23}$$

which then is solved for in the context of an integral equation over our domain.

$$\iiint F_E(\mathbf{v}, \mathbf{E}) = 0 \tag{4.24}$$

The test function can be any function and Equations (4.23) and (4.24) still hold, because we have multiplied the test function with an expression that was zero and then integrated the expression that was zero.

What we gain from this formulation is not obvious at first glance, but this opens up the possibility to split the integral equations into multiple smaller sections, or "elements". Each element gets its own test function and the value of **E** we want to solve for is approximated by a set of basis functions. The basis functions assume different types of shapes over the element and are therefore also named shape functions. The purpose of the shape functions is to be able to describe the solution over the element and therefore also need to form a complete basis over the geometry. The weight functions are chosen depending on the implementation, but a common choice is based on the Galerkin method [64] [58], which is why we sometime see this name when people are referring to FEM or finite differences.

As an example to illustrate this point we can in Figure 4.3 see a 1D example of how an arbitrary function $u(x)$ can be approximated with different basis functions for different element sizes. Here the basis functions are chosen to be the simplest form of piecewise linear. This example also highlights that we then can choose elements so they have a smaller size where the solution changes a lot, while we can have a bigger element size where the solution is more constant, which means that we can keep the DOF down and solve for the system faster.

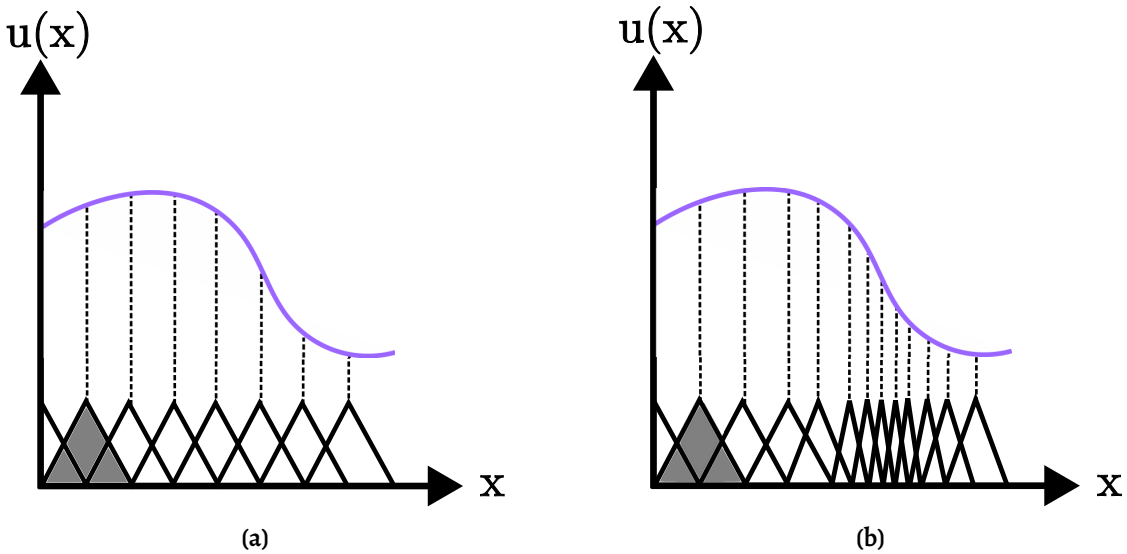

Figure 4.3: Example of how an arbitrary function u(x) is described by means of basis functions over different element partitions. The first basis function is coloured grey. In Figure 4.3a, the elements have equal size and in Figure 4.3b the elements are refined in regions where u varies more.

4.2.2 Boundary conditions

When we simulate electromagnetic fields over a domain, we need to be able to confine the size of the geometry. Electromagnetic interactions in a lossless medium stretches to infinity so there is a need for us to accurately handle wave propagation when it 'leaves' the structure so we do not get unwanted numerical artefacts and can save computation time. In the following subsections, we will present the boundary conditions needed to solve for wave propagation in an optical waveguide. We will treat periodic conditions, perfect magnetic/electric conductor, and scattering boundary conditions. The boundary conditions are discussed from the viewpoint of use in COMSOL [63], but the principle is the same for other implementations.

4.2.2.1 Perfect electric/magnetic conductor - PEC/PML

When we want to simulate interactions with an ideal metal, we can simulate a perfect electrical or magnetic boundary. This is useful when we are interested in capturing effects of ground planes or metallic effects where we do not need to account for metallic losses.

The boundary condition for a perfect electrical conductor (PEC) simply imposes the boundary condition

$$\mathbf{n} \times \mathbf{E} = 0 \tag{4.25}$$

along the boundary. Here $\mathbf{n}$ is the normal vector to the boundary. This also results in that we get a perfect symmetry plane for magnetic fields.

In a similar way the perfect magnetic conductor (PMC) can be used to create a symmetry plane for electric fields by imposing the boundary condition

$$\mathbf{n} \times \mathbf{H} = 0. \tag{4.26}$$

This means that if we are interested in simulating modes in a waveguide we can use these boundaries to create symmetry planes if the device allows for it. So if we want to simulate transverse electric modes in a waveguide that is homogeneous or has a symmetry around the the longitudinal propagation we only need to simulate half of the geometry if we add a PMC in the middle, as shown in Figure 4.4. The side effect of this choice is that we then exclude the transverse magnetic modes, since they won't appear due to the added boundary. If we instead were to use PEC, we would calculate the magnetic modes.

4.2.2.2 Periodic Floquet boundary conditions

Floquet boundary conditions are a set of boundary conditions that uses Floquet theory named after Gaston Floquet who studied these systems during the late nineteenth century [65]. It describes systems where we can express a vector field at a destination $\mathbf{x}$ as

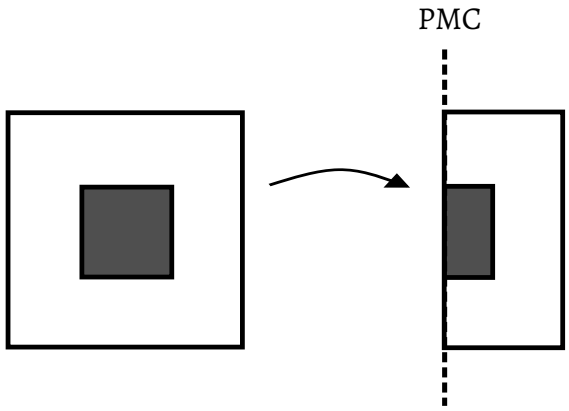

Figure 4.4: Figure showing the use of PMC to create a symmetry plane to cut the simulation domain in half.

a phase shift operation acting on a the vector field from the start

$$u_{destination} = u_{source} e^{-i\mathbf{k}_F \cdot \mathbf{x}} \tag{4.27}$$

In a normal periodic problem when we have a unit cell with length

$$L = |\mathbf{r}_{dst} - \mathbf{r}_{src}|, \tag{4.28}$$

we would have a boundary condition stating

$$u(L) = u(0). \tag{4.29}$$

If we instead have accrued a change in phase and amplitude, we can express the periodicity like in Equation (4.27) as

$$u(L) = u(0) e^{-i\mathbf{k}_F \cdot (\mathbf{r}_{dst} - \mathbf{r}_{src})}. \tag{4.30}$$

This boundary condition is useful when we want to simulate an infinite periodic structure, as described in Section 2.3, and we know that the change after the wave has propagated one unit cell results in an added phase shift.

4.2.2.3 Scattering boundary conditions

When we have a wave exiting our domain of interest, we want a way to make this wave 'go away' so it does not disturb the rest of the simulation. There are different ways to handle this such as with perfectly matched layers (PML) [66, 67], which is a well established method to truncate a simulation volume. It does come with a performance penalty and requires an additional region to be meshed to enclose the simulated volume.

Another less costly method is the scattering boundary condition (SBC) of the first-order [63]

$$\mathbf{n} \times (\nabla \mathbf{E}) - ik\mathbf{n} \times (\mathbf{E} \times \mathbf{n}) = 0, \tag{4.31}$$

which is a complex-valued variation on the Robin boundary condition [68, 69]. This can be made more effective by including a second-order term with an added computational cost. The second-order scattering boundary condition adds a tangential derivative term along the boundary which lessens reflection at greater angles of incidence.

$$\mathbf{n} \times (\nabla \mathbf{E}) - ik\mathbf{n} \times (\mathbf{E} \times \mathbf{n}) - \frac{1}{2ik_0} \nabla \times (\mathbf{n} \cdot (\nabla \times \mathbf{E})) = 0. \tag{4.32}$$

All of these methods still allow reflections to occur when the incidence angle of the field deviated from the boundary normal. In many cases the SBC is good enough but it depends on the geometry and scattering properties of the specific problem we try to solve.

4.2.3 Eigenmode simulations

When we have a periodic Bloch structure, as described in Sections 2.3 and 4.2.2.2, we often find ourselves in a situation where we want to calculate the dispersion relation with respect to frequency. The older conventional way to numerically achieve this, as described in, for instance, Refs. [70][71], is to solve for the eigenmodes of the system. We fix the wave vector k and solve for which frequencies the eigenmodes have. Then we perform a parametric sweep of the wave vector to get the full dispersion. In some instances, however, it is more interesting to do this the other way around and fix the frequency instead of k. We might, for example, be interested in a design that only can operate at certain frequencies. Approaches to achieve this in 2D with FEM was first proposed in Refs [72] and [73], but generalised formally in 3D by [74].

The process to get the wave vector at a specified frequency with finite element eigenmode simulation involves a rewrite of the weak expression presented in Equation (4.23). The way we do this is rather straight forward, we express the electric field as a periodic vector field in a similar way as in the case for the Floquet boundary condition:

$$\mathbf{E}(\mathbf{x}) = \mathbf{u}(\mathbf{x}) e^{i(\omega t - \mathbf{k} \cdot \mathbf{x})}, \tag{4.33}$$

Where $u(\mathbf{x}$ is a periodic function. We then insert Equation (4.33) into the wave Equation (4.22) and receive a new field equation of $\mathbf{u}$:

$$\frac{k^2}{\mu}\mathbf{u} - \frac{k}{\mu}(\mathbf{k} \cdot \mathbf{u}) - i\mathbf{k} \times \left(\frac{1}{\mu}\nabla \times \mathbf{u}\right) - i\nabla \times \left(\frac{1}{\mu}\mathbf{k} \times \mathbf{u}\right) + \nabla \times \left(\frac{1}{\mu}\nabla \times \mathbf{u}\right) - \varepsilon\frac{\omega^2}{c^2}\mathbf{u} = 0. \tag{4.34}$$

We can then solve for $\mathbf{k}$ like an eigenvalue problem, by writing $\mathbf{k} = \lambda \cdot \hat{\mathbf{r}}$, where $\hat{\mathbf{r}}$ is the normalised direction of periodicity and λ is the eigenvalue we solve for. We need to fix the periodic direction, $\hat{\mathbf{r}}$, in order to decrease the dimension of $\mathbf{k}$ down to 1 so that we can solve for it using an eigenvalue solver.

To be able to solve it, we need to use Equation (4.34) to create a new weak formulation for the finite element solver. This is done by multiplying Equation (4.34) with a test function $\mathbf{v}$:

$$F_E(\mathbf{v}, \mathbf{u}) = \frac{k^2}{\mu}\mathbf{v} \cdot \mathbf{u} - \frac{1}{\mu}(\mathbf{v} \cdot \mathbf{k})(\mathbf{k} \cdot \mathbf{u}) - i\frac{1}{\mu}\mathbf{v} \cdot [\mathbf{k} \times (\nabla \times \mathbf{u})] - i(\nabla \times \mathbf{v}) \cdot \frac{1}{\mu}(\mathbf{k} \times \mathbf{u}) \tag{4.35}$$
$$+ (\nabla \times \mathbf{v}) \cdot \frac{1}{\mu}(\nabla \times \mathbf{u}) - \varepsilon\frac{\omega^2}{c^2}\mathbf{v} \cdot \mathbf{u} = 0.$$

So if we are interested in the propagation constant along the propagation in the z direction, along a periodic structure, we simply use the expression (4.35) and set the k-vector to be $\mathbf{k} = \lambda\hat{z}$ and solve the expression for eigenvalue λ.

5

Summary of papers

Paper I

Adaptive meshing strategies for nanophotonics using a posteriori error estimation

In Paper I we present a meshing strategy for simulating nanophotonic systems using a posteriori error estimation in finite element methods. By first simulating the electric field on an initial course mesh, we can then use this field to evaluate the a posteriori errors for each element in a finite element mesh. Using this information, we can then determine which of these elements exhibit the largest errors. By having a scheme where we iteratively only refine a fraction of the total elements and only choosing the elements that show the largest errors we provide a h-FEM method that reliably and predictably converges to a result while keeping the DOF down as much as possible.

We implement this strategy in COMSOL Multiphysics for arbitrary 3D geometries and benchmark the strategy against other conventional adaptive meshing approaches. We demonstrate that the use of adaptive meshing leads to faster convergence with lower memory footprint for complex three-dimensional nanophotonic structures. Further we discuss an issue with mesh refinement where propagation of mesh refinement can result in poor convergence for situations where the starting mesh is to course.

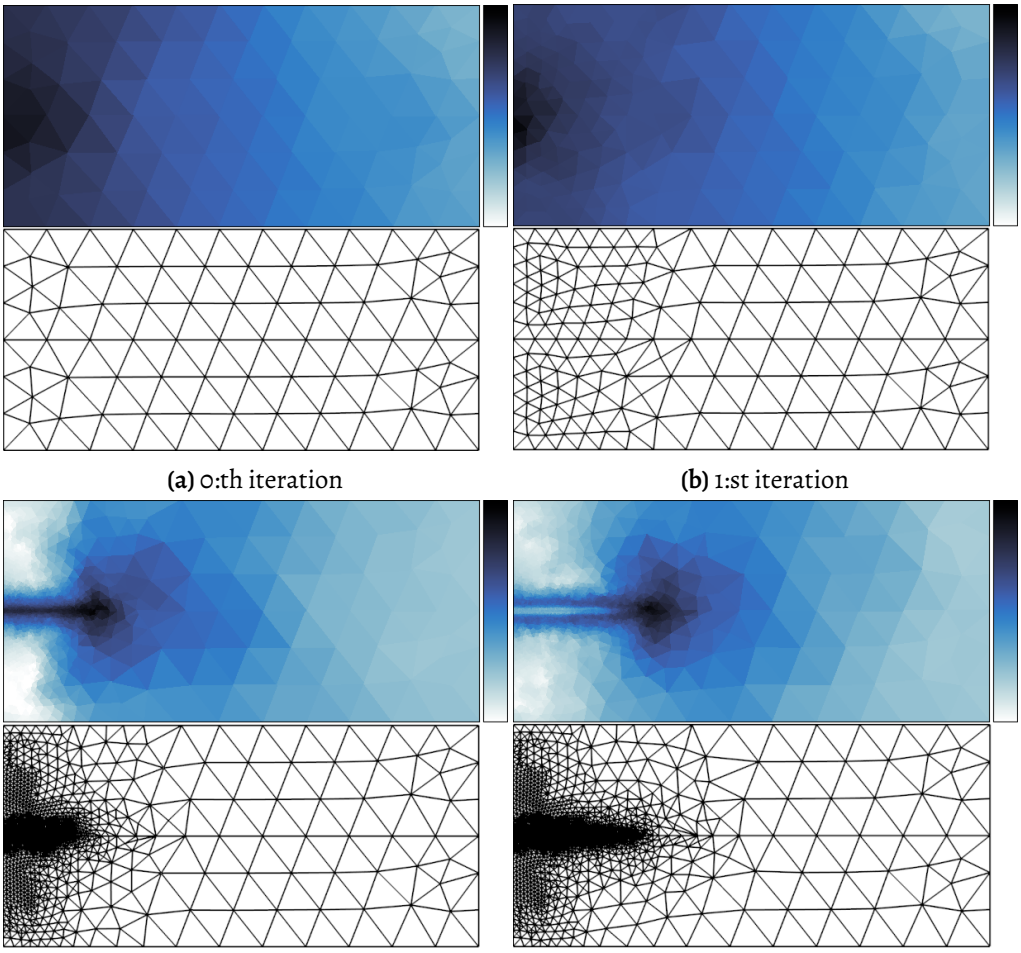

(a) 0:th iteration **(b)** 1:st iteration

(c) 5:th iteration **(d)** 10:th iteration.

Figure 5.1: Mesh progression starting from a very coarse mesh. A horizontal surface charge is present in the middle of the structure. The mesh is not fine enough to propagate the plasmon to the right, so the refinement gets stuck in the early iterations. The top part of each panel shows the mesh element error in logarithmic scale and the bottom figures show the actual mesh.

6

Conclusions and outlook

We have now reached the beginning, for surely this is not the end of this journey? We have over the course of this thesis learnt and reviewed the development of the field of nonlinear optics. A development that is the result of centuries of progress. We have learned how dielectric materials behave under the influence of electric fields. How these fields can be controlled and guided to create the effects we want. When we now stop at this thesis, we have the computational knowledge to simulate these effects, being able to guide the light. Where do we go from here?

We have now reached the final vantage point of this thesis where I will stop a bit and look forward from this position. In the grand scheme of things, the subject of nonlinear physics is a rather new field, but also quite old, emerging during the 1900s resting comfortable on the shoulders of electromagnetism and quantum physics. The basic physics has been well studied now for some generations. Yet the field is thriving and expanding at the moment. Our technology in lasers and manufacturing of photonic devices has now improved to such a point that we now can manufacture many things that previously was unthinkable. The possibility to use 2020s lithography techniques (now called "modern") developed much for the purpose of current electronics manufacturing opens up the door for amazing materials design. We can now construct optical amplification below conventional quantum limits [1] with on chip manufacturing 55 years after Miller coined the term integrated optics [75], a testament to the quality of today's manufacturing. Yet another field has truly emerged based on the same possibility brought from better computational methods and manufacturing and that is the field of metamaterials [76].

With increasing manufacturing prowess, we can now design materials that have much more desirable characteristics than what nature typically provides. With increasing computational abilities, we now have the possibility to combine it all and create specific materials based on our needs on a case-by-case basis. So-called inverse design of

materials, where instead of predicting how a specific material will behave we design it ourselves to behave as we want.

Acknowledgments

Many people really deserve to be mentioned for the feedback and support they have given me during this work and I would like to thank you all for your assistance. I specifically would like to thank my supervisor Philippe for the insights and lighthearted discussions that led up to this thesis. I'd also like to thank my girlfriend Ingrid who, both put up with me during my working frenzy and also supported me and gave me continuous feedback.

Bibliography

[1] Z. Ye, P. Zhao, K. Twayana, M. Karlsson, V. Torres-Company, and P. A. Andrekson, *Overcoming the quantum limit of optical amplification in monolithic waveguides,* Science Advances **7**, eabi8150 (2021). doi:10.1126/sciadv.abi8150.

[2] J. W. Choi, B.-U. Sohn, E. Sahin, G. F. R. Chen, P. Xing, D. K. T. Ng, B. J. Eggleton, and D. T. H. Tan, *An optical parametric Bragg amplifier on a CMOS chip,* Nanophotonics **10**, 3507 (2021) [cited 2024-08-01]. doi:10.1515/nanoph-2021-0302.

[3] D. J. Griffiths, *Introduction to Electrodynamics* (Cambridge University Press, 2023).

[4] J. D. Jackson, *Classical electrodynamics* (New York, NY: Wiley, 1999). ISBN 9780471309321.

[5] A. Yariv and P. Yeh, *Optical Waves in Crystals: Propagation and Control of Laser Radiation* (New York, NY: Wiley, 2003). ISBN 0471430811.

[6] J. l. R. d'Alembert, *Recherches Sur La Courbe Que Forme Une Corde* (Deutsche Akademie der Wissenschaften zu Berlin, 1747).

[7] J. l. R. d'Alembert, *Suites Des Recherches Sur La Courbe Que Forme Une Corde* (Deutsche Akademie der Wissenschaften zu Berlin, 1747).

[8] J. l. R. d'Alembert, *Addition Au Memoire Sur La Courbe Que Forme Une Corde* (Deutsche Akademie der Wissenschaften zu Berlin, 1750).

[9] L. Euler, *De la propagation du son,* Mémoires de l'académie des sciences de Berlin , (1759). https://archive.org/details/euler-e305.

[10] J. L. d. Lagrange, *Nouvelles recherches sur la nature et la propagation du son* (Gauthier-Villars, 1760).

[11] J. C. Maxwell, *VIII. A dynamical theory of the electromagnetic field,* Philosophical Transactions of the Royal Society of London **155**, 459 (1865). doi:10.1098/rstl.1865.0008.

[12] H. Hertz, *Electric Waves: Being Researches on the Propagation of Electric Action with Finite Velocity Through Space* (Dover Publications, 1893). ISBN 9780486600574.

[13] O. Heaviside, *Electromagnetic Theory* ("The Electrician" printing and publishing Company, 1893).

[14] O. Heaviside, *Electromagnetic Theory. Oliver Heaviside. Complete and Unabridged Edition of Volume I … II and III with a Critical and Historical Introduction by Ernst Weber …* (Dover publications, 1950).

[15] J. Liu, *Photonic Devices* (Cambridge University Press, 2009). ISBN 9781139441148.

[16] B. E. A. Saleh and M. C. Teich, *Nonlinear Optics*. In , *Fundamentals of Photonics* (John Wiley & Sons, Ltd, 1991). doi:10.1002/0471213748.ch19.

[17] P. Markos and C. M. Soukoulis, *Wave propagation: from electrons to photonic crystals and left-handed materials* (Princeton University Press, 2008).

[18] C. Kittel, *Introduction to Solid State Physics* (Wiley, 2004). ISBN 9780471415268.

[19] N. Ashcroft and N. Mermin, *Solid State Physics* (Cengage, 2021). ISBN 9780357670811.

[20] F. Bloch, *Über die Quantenmechanik der Elektronen in Kristallengittern,* Zeitschrift für Physik **52**, 555 (1929). doi:10.1007/BF01339455.

[21] J. M. Ziman, *Principles of the Theory of Solids* (Cambridge University Press, 1972).

[22] J. V. Moloney and A. C. Newell, *Nonlinear Optics* (Westview Press, 2004). ISBN 0-8133-4118-3.

[23] R. W. Boyd, ed., *Nonlinear Optics (Third Edition)* (Burlington: Academic Press, 2008). ISBN 978-0-12-369470-6. doi:10.1016/B978-0-12-369470-6.00020-4.

[24] N. Bloembergen, *Nonlinear Optics* (World Scientific, 1996). doi:10.1142/3046.

[25] ISPNLO, *International School on Parametric Nonlinear Optics,* https://www.youtube.com/@ispnlo9041/, 2015.

[26] P. N. Butcher and D. Cotter, *The Elements of Nonlinear Optics* (Cambridge University Press, 1990).

[27] A. Einstein, *Die Grundlage der allgemeinen Relativitätstheorie,* Annalen der Physik **354**, 769 (1916). doi:10.1002/andp.19163540702.

[28] P. Dirac, *The Principles of Quantum Mechanics* (Clarendon Press, 1981). ISBN 9780198520115.

[29] G. B. Arfken, H. J. Weber, and F. E. Harris, *Mathematical Methods for Physicists* (Boston: Academic Press, 2013). ISBN 978-0-12-384654-9. doi:10.1016/B978-0-12-384654-9.00011-6.

[30] P. A. Franken, A. E. Hill, C. W. Peters, and G. Weinreich, *Generation of Optical Harmonics,* Phys. Rev. Lett. **7**, 118 (1961). doi:10.1103/PhysRevLett.7.118.

[31] W. Kaiser and C. G. B. Garrett, *Two-Photon Excitation in CaF_2: Eu^{2+}*, Phys. Rev. Lett. **7**, 229 (1961). doi:10.1103/PhysRevLett.7.229.

[32] M. Göppert-Mayer, *Über Elementarakte mit zwei Quantensprüngen,* Annalen der Physik **401**, 273 (1931). doi:10.1002/andp.19314010303.

[33] R. W. Terhune, P. D. Maker, and C. M. Savage, *Optical Harmonic Generation in Calcite,* Phys. Rev. Lett. **8**, 404 (1962). doi:10.1103/PhysRevLett.8.404.

[34] J. A. Armstrong, N. Bloembergen, J. Ducuing, and P. S. Pershan, *Interactions between Light Waves in a Nonlinear Dielectric,* Phys. Rev. **127**, 1918 (1962). doi:10.1103/PhysRev.127.1918.

[35] J. E. Midwinter and J. Warner, *The effects of phase matching method and of uniaxial crystal symmetry on the polar distribution of second-order non-linear optical polarization,* British Journal of Applied Physics **16**, 1135 (1965). doi:10.1088/0508-3443/16/8/312.

[36] M. V. Hobden, *Phase-Matched Second-Harmonic Generation in Biaxial Crystals,* Journal of Applied Physics **38**, 4365 (1967). doi:10.1063/1.1709130.

[37] D. S. Hum and M. M. Fejer, *Quasi-phasematching,* Comptes Rendus Physique **8**, 180 (2007). doi:10.1016/j.crhy.2006.10.022.

[38] S. ning Zhu, Y. yuan Zhu, and N. ben Ming, *Quasi-Phase-Matched Third-Harmonic Generation in a Quasi-Periodic Optical Superlattice,* Science **278**, 843 (1997). doi:10.1126/science.278.5339.843.

[39] R. L. Byer, *Quasi-Phasematched Nonlinear Interactions and Devices,* Journal of Nonlinear Optical Physics & Materials **06**, 549 (1997). doi:10.1142/S021886359700040X.

[40] J. S. Pelc, C. R. Phillips, D. Chang, C. Langrock, and M. M. Fejer, *Efficiency pedestal in quasi-phase-matching devices with random duty-cycle errors,* Opt. Lett. **36**, 864 (2011). doi:10.1364/OL.36.000864.

[41] M. Fejer, G. Magel, D. Jundt, and R. Byer, *Quasi-phase-matched second harmonic generation: tuning and tolerances,* IEEE Journal of Quantum Electronics **28**, 2631 (1992). doi:10.1109/3.161322.

[42] G. Agrawal, *Nonlinear Fiber Optics* (Elsevier Science, 2019). ISBN 9780128170434.

[43] S. E. Harris, M. K. Oshman, and R. L. Byer, *Observation of Tunable Optical Parametric Fluorescence,* Phys. Rev. Lett. **18**, 732 (1967). doi:10.1103/PhysRevLett.18.732.

[44] W. H. Louisell, A. Yariv, and A. E. Siegman, *Quantum Fluctuations and Noise in Parametric Processes. I.,* Phys. Rev. **124**, 1646 (1961). doi:10.1103/PhysRev.124.1646.

[45] C. M. Caves, *Quantum limits on noise in linear amplifiers,* Phys. Rev. D **26**, 1817 (1982). doi:10.1103/PhysRevD.26.1817.

[46] S. Obayya, *Computational Photonics* (Wiley, 2011). ISBN 978-1-119-95750-8.

[47] E. Schrödinger, *An Undulatory Theory of the Mechanics of Atoms and Molecules,* Phys. Rev. **28**, 1049 (1926). doi:10.1103/PhysRev.28.1049.

[48] R. Y. Chiao, E. Garmire, and C. H. Townes, *Self-Trapping of Optical Beams,* Phys. Rev. Lett. **13**, 479 (1964). doi:10.1103/PhysRevLett.13.479.

[49] l. D. Landau and V. L. Ginzberg, *On the theory of superconductivity,* JETP **20**, (1950).

[50] L. D. Landau, *73 - On the theory of superconductivity,* in *Collected Papers of L.D. Landau*, edited by D. TER HAAR (Pergamon, 1965), p. 546. doi:10.1016/B978-0-08-010586-4.50078-X.

[51] M. E. Marhic, *Fiber Optical Parametric Amplifiers, Oscillators and Related Devices* (Cambridge University Press, 2007).

[52] R. Y. Chiao, E. Garmire, and C. H. Townes, *Self-Trapping of Optical Beams,* Phys. Rev. Lett. **13**, 479 (1964). doi:10.1103/PhysRevLett.13.479.

[53] A. Hasegawa and F. Tappert, *Transmission of stationary nonlinear optical pulses in dispersive dielectric fibers. II. Normal dispersion,* Applied Physics Letters **23**, 171 (1973). doi:10.1063/1.1654847.

[54] F. D. Tappert and C. N. Judice, *Recurrence of Nonlinear Ion Acoustic Waves,* Phys. Rev. Lett. **29**, 1308 (1972). doi:10.1103/PhysRevLett.29.1308.

[55] J. Fleck, J. R. Morris, and M. D. Feit, *Time-dependent propagation of high energy laser beams through the atmosphere,* Applied Physics **10**, 129 (1976). doi:10.1007/BF00896333.

[56] R. Courant, *Variational methods for the solution of problems of equilibrium and vibrations,* Bull. Am. Math. **49**, 1 (1943). doi:10.1090/S0002-9904-1943-07818-4.

[57] J.-M. Jin, *The Finite Element Method in Electromagnetics* (Wiley, 2014). ISBN 978-1-118-57136-1.

[58] N. Ottosen and H. Petersson, *Introduction to the Finite Element Method* (Prentice-Hall, 1992). ISBN 0-13-473877-2.

[59] *Comsol Multiphysics Reference Manual, pp. 1422-1440. COMSOL Multiphysics® v. 6.2. COMSOL AB, Stockholm, Sweden. 2024",.*

[60] *Comsol Multiphysics Reference Manual, pp. 1268-1342. COMSOL Multiphysics® v. 6.2. COMSOL AB, Stockholm, Sweden. 2024",*.

[61] https://www.comsol.com/multiphysics/finite-element-method.

[62] A. J. Svärdsby and P. Tassin, *Adaptive meshing strategies for nanophotonics using a posteriori error estimation,* Opt. Express **32**, 24592 (2024). doi:10.1364/OE.523907.

[63] *COMSOL Multiphysics,* Stockholm, Sweden, 2022. https://www.comsol.com/.

[64] B. Galerkin, *"On electrical circuits for the approximate solution of the Laplace equation",* Vestnik Inzh , 897 (1915).

[65] G. Floquet, *Sur les équations différentielles linéaires à coefficients périodiques,* Annales scientifiques de l'École Normale Supérieure **2e série, 12**, 47 (1883). doi:10.24033/asens.220.

[66] S. G. Johnson, *Notes on Perfectly Matched Layers (PMLs),* 2021. https://arxiv.org/abs/2108.05348.

[67] J.-P. Berenger, *A perfectly matched layer for the absorption of electromagnetic waves,* Journal of Computational Physics **114**, 185 (1994). doi:10.1006/jcph.1994.1159.

[68] G. Robin, *Sur la distribution de l'électricité à la surface des conducteurs fermés des conducteurs ouverts,* Annales scientifiques de l'École Normale Supérieure **3**, 3 (1886). http://eudml.org/doc/80956.

[69] K. Gustafson and T. Abe, *The third boundary condition - was it Robin's?,* The matematical Intelligencer , 63 (1998). doi:10.1007/BF03024402.

[70] J. D. Joannopoulos, S. G. Johnson, J. N. Winn, and R. D. Meade, *Photonic Crystals: Molding the Flow of Light - Second Edition* (Princeton University Press, 2008). ISBN 9780691124568. doi:10.2307/j.ctvcm4gz9.

[71] K. Sakoda, *Optical Properties of Photonic Crystals* (Springer Berlin, Heidelberg, 2005). ISBN 978-3-642-42408-3. doi:10.1007/b138376.

[72] M. Davanço, Y. Urzhumov, and G. Shvets, *The complex Bloch bands of a 2D plasmonic crystal displaying isotropic negative refraction,* Opt. Express **15**, 9681 (2007). doi:10.1364/OE.15.009681.

[73] C. Engström, C. Hafner, and K. Schmidt, *Computations of lossy Bloch waves in two-dimensional photonic crystals,* Journal of Computational and Theoretical Nanoscience **6**, 775 (2009). doi:10.1166/jctn.2009.1108.

[74] C. Fietz, Y. Urzhumov, and G. Shvets, *Complex k band diagrams of 3D metamaterial/photonic crystals.,* Opt. Express **19**, 19027 (2011). doi:10.1364/OE.19.019027.

[75] S. E. Miller, *Integrated Optics: An Introduction,* Bell System Technical Journal **48**, 2059 (1969). doi:10.1002/j.1538-7305.1969.tb01165.x.

[76] A. Krasnok, M. Tymchenko, and A. Alù, *Nonlinear metasurfaces: a paradigm shift in nonlinear optics,* Materials Today **21**, 8 (2018). doi:10.1016/j.mattod.2017.06.007.

Paper I

Adaptive meshing strategies for nanophotonics using a posteriori error estimation
Albin J. Svärdsby and Philippe Tassin
Optics Express **32**, 14, pp. 24592-24602 (2024) doi: 10.1364/OE.523907